

Monitoring NuMI Target

Alexei Kulik, University of Pittsburgh/FNAL

Monitoring the target is one of the challenges NuMI project is facing. The target has to operate at $4 \cdot 10^{13}$ protons per 1 ms spill which comes to $4 \cdot 10^{16}$ p/s. The 90° charged particles flux amounts to 10 GHz/cm² 1.5 meters away from the target which creates an apparent problem for the counting technique. This paper is a preliminary study of the various target monitoring techniques.

1 Budal

This technique developed at CERN back in 60-th[1] employs the effect of δ - rays escaping a target thus resulting in target's positive charge. The electrical circuit is shown in Fig. 1. Positive bias is recommended to trap soft (~ 50 eV) electrons at the target's surface. If not trapped, these will contribute to the total charge in a poor-controlled fashion affecting both linearity and repeatability. A relay restores base potential before the next spill. The NuMI target has both favourable geometry and material for producing a high output signal. A thin cylinder oriented along the beam line provides high probability for δ -electrons to escape, so does the light material (Beryllium or Graphite). Such conditions may result in a signal of 10-15 elementary charges per incident proton. It comes to 35 Volt for 1 μ F integrating capacitor. The response is reported to be linear, without saturation and repeatable. Insulation is strongly recommended for the targets operating in air in order to prevent uncontrolled recombination of airborne carriers at the target's surface.

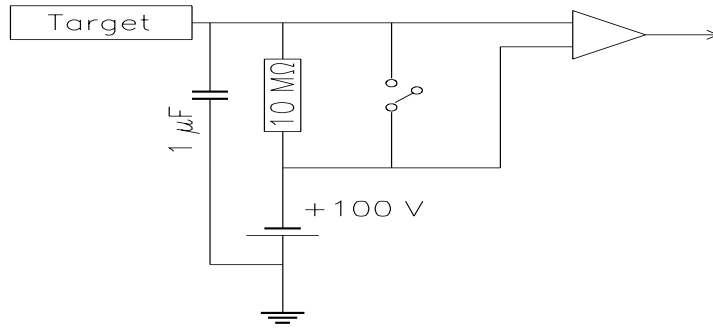


Figure 1: Measurement of the induced charge.

Along with the attractive features listed above, this technique has an apparent disadvantage: it possesses a potential danger of material failure under high radiation exposure. The classical work [1] is of little help here since it reports the results of tests below 10^{12} protons/pulse. FNAL experience at $3 \cdot 10^{12}$ /pulse (the beamline for E773,E779 in 1990-91) is discouraging: 4 targets have been made and exposed one after one, all 4 did work properly in the beginning and all 4 failed after about a month of exposition. The reason is not known since during an exposition a target becomes too hot to be inspected by a human. The NuMI radiation environment will be far more hostile than that. The bottomline is that we need a solid study of the various materials under high radiation which we can not afford. The one who bets on this technique is taking a risk of a series of mysterious failures without a possibility to figure out the reason. Unless he has an access to the nuclear engineering or defence research files.

2 Counting Technique

Although 10 GHz/cm^2 sounds hopeless let's give it a second thought. One may think of employing Čerenkov counters which are blind to a soft part of radiation. Gas counter with its high threshold of $\gamma = 20 - 100$ should count at a far lower rate than the traditional scintillator. Glass Čerenkov counter can be made of 1 mm dia. Furthermore a possibility of the amplitude discrimination promises both further rate reduction and suppression of the secondary interaction products, in particular, electrons. And, at last, who told that it must be a hole all the way through the shielding? Yes, plugging a hole increases scattering and makes you less sure that what you see comes directly from the target. However, let's get the numbers and then weigh odds and evens. It will be convenient for me to address these 3 issues in a different and even mixed order.

2.1 Plugging a hole

Fig. 2, top shows traditional 90° geometry with a hole bored in the iron shielding. What if one partially plugs a hole as in lower picture? Line 'Total' of table 1 gives a rough idea of the rate. The rates are in MHz/cm^2 , plug material is iron.

Table 1. Effect of Plugging the Hole.

	Open Hole	5 cm Plug	15 cm Plug
Total	5000	200	28
$\gamma > 2$	1800	130	18
$\gamma > 40$	525	16	3
$\gamma > 40, \alpha < 0.05$	450	14	0.055
Events Generated	$0.273 \cdot 10^6$	$1.579 \cdot 10^7$	$2.1 \cdot 10^7$
Ampl. Fact.	400	$2.5 \cdot 10^6$	$2.5 \cdot 10^6$
POT	$1.092 \cdot 10^8$	$3.95 \cdot 10^{13}$	$5.25 \cdot 10^{13}$
1 Event Worth	75 MHz/cm^2	32.3 kHz/cm^2	27 kHz/cm^2
File	air_2.5cm_10fi	yield_2_10_plug5	yield_2_10_plug15

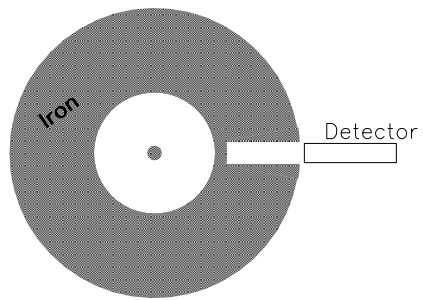
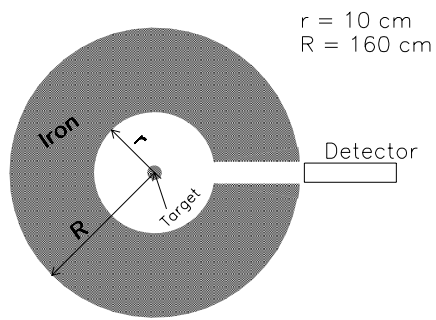


Figure 2: 90° monitor: open hole (upper) and plugged hole (lower).

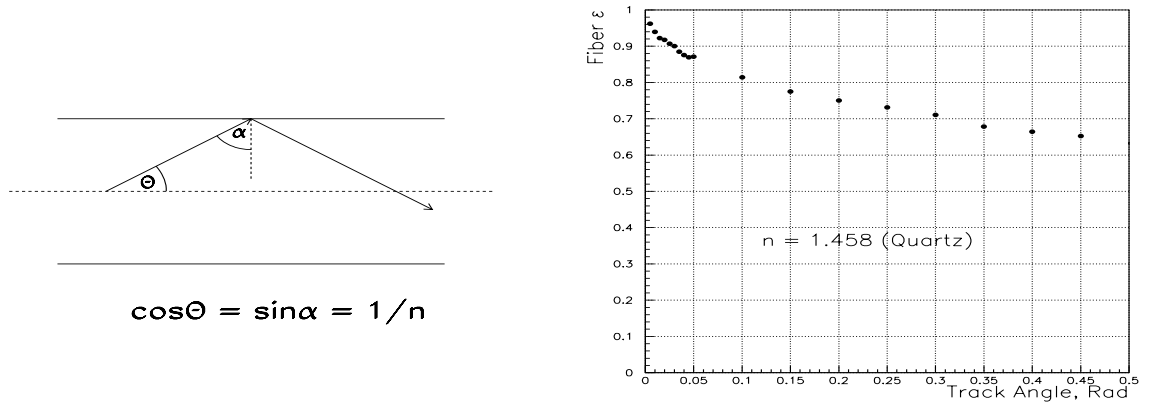


Figure 3: Left: Propagation of the Čerenkov light through the optical fiber. Right: Light collection efficiency as a function of the track angle.

The observation one can make from Table 1 is that the flux gets reduced dramatically even by a thin plug. The reason is multiple scattering. A particle of say 300 MeV momentum would scatter in 5 cm of iron through

$$\Theta = \frac{14 \text{ MeV}}{300 \text{ MeV}} \sqrt{5 \text{ cm}/1.76 \text{ cm}} = 78 \text{ mrad}. \quad (1)$$

If it is more than the hole aspect ratio (diameter/length) then so heavily scattered particle just can not do it through the hole. The numbers in the table 1 are for the hole of 1 cm diameter 150 cm length, so this is just the case.

Skip the rest of the table 1 by now, it will make sense later in this paper.

2.2 Glass Čerenkov Counter

View a piece of quartz fiber with a phototube and make a Čerenkov counter. For the fast particle travelling along the fiber axis, radiation angle matches exactly total internal reflection angle (Fig. 3, left) thus the Čerenkov light would propagate through the fiber. Fig. 3, right shows light collection efficiency as a function of the track angle

with respect to the fiber axis (averaged over the track entry point and azimuth angle).

The advantages of this technique are quite clear:

- It can be made very small (1 mm) thus reducing the surface and rate.
- Excellent spectral transmittance together with perfect light collection will give 60 photoelectrons per cm. For 10 cm length it is 600 p.e. or $\sigma = 4\%$ amplitude resolution.
- Because of good amplitude resolution, amplitude discrimination can be applied efficiently. This will select only the particles quite parallel to the counter axis and fast enough to stay above Čerenkov threshold after passing 10 cm of glass. The rate of such will be far below the overall rate and particles directly from target are likely to dominate. If this turns true, no coincidence required: a single counter will do the job of monitoring.

Optical quartz fibers of up to 1.5 mm dia. are available from 3M for \$7/meter.

2.2.1 Amplitude Spectrum

In order to produce maximal signal of 600 p.e. a particle has to make all 10 cm through the fiber. So do not contribute to high-amplitude signal the particles which are:

- Below threshold
- Getting below threshold through the ionization losses
- Non-parallel to the counter axis
- Getting out of the fiber due to multiple scattering

This makes quite a reduction. Fig. 4 shows the simulated amplitude spectra for the fibers of 1 and 2 mm dia. and 10 cm long. Open hole, neither amplitude resolution nor light collection efficiency

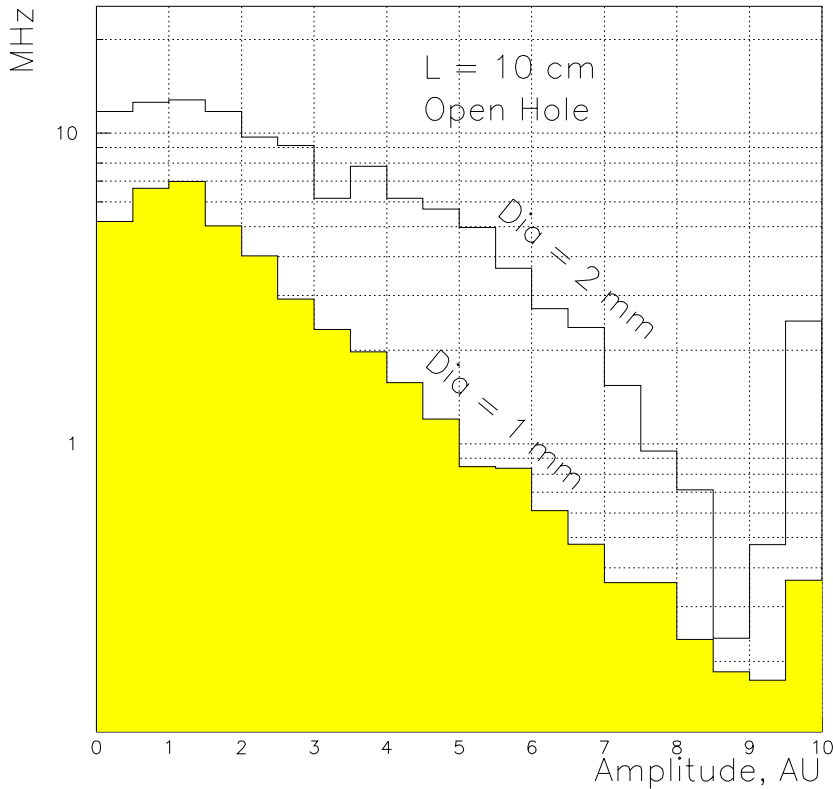


Figure 4: Čerenkov amplitude spectra for the fibers of different diameter.

yet applied. Both spectra show a high-amplitude peak of the order of a MHz. Note that smaller diameter results not only in less rate but also in stronger amplitude discrimination because less fraction of the incident particles can meet more stringent requirements (mostly on multiple scattering) to produce a maximal signal.

Fig. 5 gives some idea about the origin of the peak. Left picture shows the amplitude spectrum for 2 mm dia, 10 cm long fiber and 5 cm thick plug. Shaded histogram is the contribution by electrons. Apparently electrons are not responsible for the peak, it is produced exclusively by hadrons and muons. Good. Then the right picture shows the angular distribution for the particles making a peak (Ampl

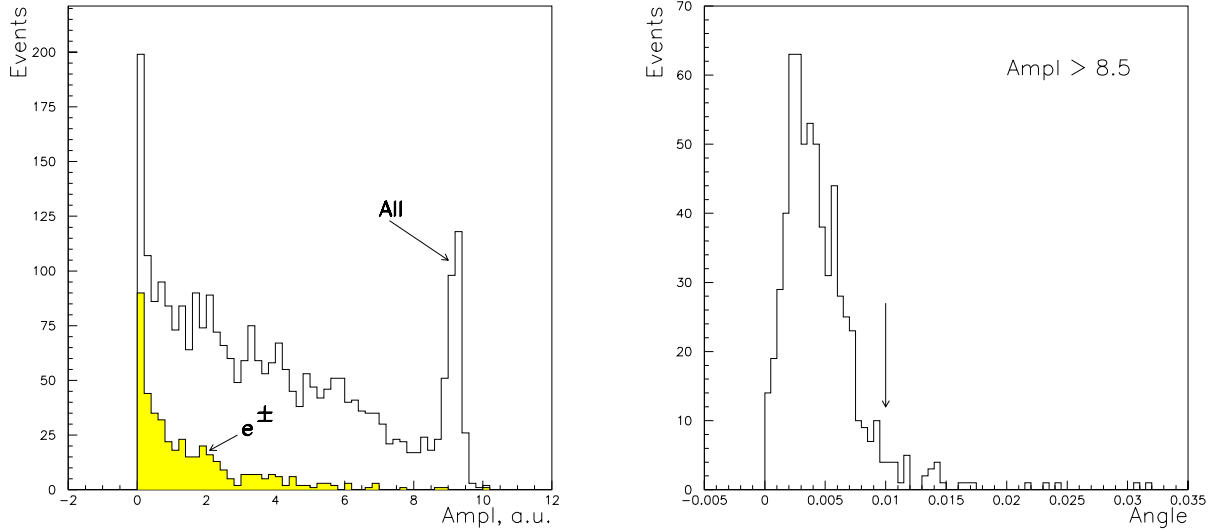


Figure 5: Left: Amplitude spectrum convoluted with light collection efficiency from fig.3. Electrons do not contribute to the peak. Right: Angular distribution for the particles in the peak area (Ampl > 8.5). Arrow indicates detector aspect ratio = radius/length.

> 8.5). Arrow shows the aspect ratio of the detector, 1 mm/10 cm. If you assume a 1 cm hole bored in 150 cm thick shield it will come to about the same aspect ratio. The conclusion is that the particles contributing to the peak point back to the target within a hole aspect ratio precision. And this is good because it matches the expectations for the particles coming directly from target. Particles rescattered in the shield would normally come at higher angles and make a signal below threshold. Note that this is the case of plugged hole.

The effects to spoil the amplitude spectrum are resolution and pile-up. As the overall rate comes close to the critical value of 50 MHz (driven by bucket spacing of 19 ns), pile-up becomes non-negligible. The spectra with light collection efficiency, pile-up and resolution taken into account are shown in Fig. 6. Two geometries in question show about the same rate: 670 kHz and 850 kHz for 1 mm fiber, open hole and 2 mm fiber, plugged hole respectively at a threshold of

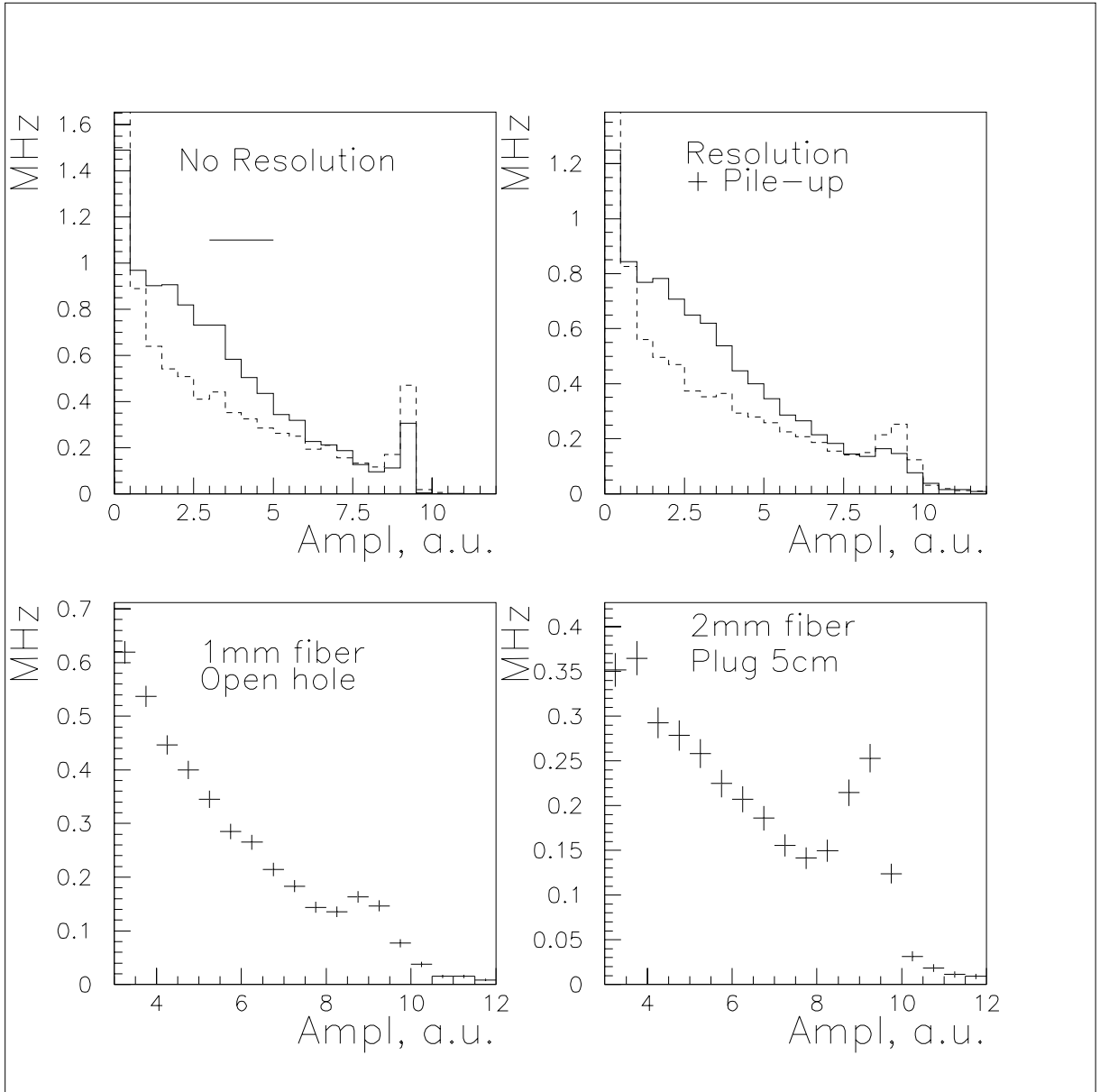


Figure 6: Glass Čerenkov amplitude spectra. Top left: ideal resolution for 1 mm fiber and open hole (solid) and 2 mm fiber and 5 cm iron plug (dashed). Top right: The same with resolution and pile-up. Bottom left: Detailed view of the peak for 1 mm, open hole. Bottom right: Detailed view for 2 mm, plugged hole.

8. The 4-fold increase in the area is compensated by plug. However, the spectrum for 2 mm fiber looks preferable. This comes from better signal-to-noise ratio in the original spectrum (top left). Compare also peak-to-valley ratio in fig.4.

There is one more effect (not shown in Fig.6) which is significant for the open hole case. The phototube diameter can not be made 1 mm, 1 cm is more realistic. So the flux through the PMT face will be ≈ 1.5 GHz. Each particle crosses 1-2 mm of the PMT window glass making a signal of 1-2% of the maximal signal. A pile-up of $1.5 \text{ GHz} \times 19 \text{ ns} = 30$ pulses per bucket worsens the resolution from 4% to 5%.

2.3 Phototubes

The candidates to the phototube for such a detector are:

Table 4. PMT Candidates

Item	Size	Window material	Rise time, ns	FWHM, ns
Hamamatsu R2496	10 mm dia.	Quartz	0.7	
Phillips XP1712,XP1714	Multianode, 2.54×2.54 mm pixels	Sapphire		8
Hamamatsu H6600-03	Multianode, 8 mm dia. divided to 4 pixels	UV Glass	0.7	
Hamamatsu H7260	Multianode, 0.8×7 mm pixels	UV Glass	0.7	

Quartz has a spectral performance superior to that of both sapphire and UV glass, however it may not be critical. The size of the multi-anode pixels matches the fiber size almost perfectly. Tiem response of 8 ns FWHM is marginal keeping in mind 19 ns bunch spacing.

Radiation hardness. PDG defines rad as

$$1 \text{ rad} = 6.24 \cdot 10^{10} \text{ MeV/kg} \quad (2)$$

which comes to

$$1 \text{ Mrad} = 4 \cdot 10^{13} \text{ MIP/cm}^2 \quad (3)$$

assuming

$$\frac{dE}{dx} = 1.56 \frac{\text{MeV} \cdot \text{cm}^2}{\text{g}^{-1}} \quad (4)$$

Assuming 10^7 seconds of continuous operation per year a peak flux of 5 GHz/cm^2 comes to

$$5 \cdot 10^9 \frac{1}{\text{s}} \times 10^{-3} \text{s} \times \frac{1}{2\text{s}} \times 10^7 \text{s} = 2.5 \cdot 10^{13} \text{ MIP/year} = 0.6 \text{ Mrad/year} \quad (5)$$

As this estimate does not account for neutrons and γ 's lets say the real doze is 10 times of that. Even then we are in a good shape. The PMT lifetime in severe radiation environment is driven by the darkening of the window. This is in turn negligible up to tens of Mrad for certain types of glass [2], in particular for quartz and UV glass [3].

As the fiber core is made of quartz, it behaves accordingly. However, clad and buffer (organic) are less hard. So it is likely that only a bare core is suitable.

2.4 problems

It is not yet clear at that point to which extent the GEANT production code may be trusted at 90^0 . Also it is not clear to which extent the cracks can be avoided in the mechanical design.

2.5 Gas Čherenkov Counter

The advantage of the gas counter is its high threshold. The disadvantages are:

- It is larger in diameter (rate) and in length.
- No amplitude discrimination because of poor photoelectron statistics.

Let's consider a 1 meter long counter with Nitrogen at atmospheric pressure. $\eta = n - 1 = 3 \cdot 10^{-4}$.

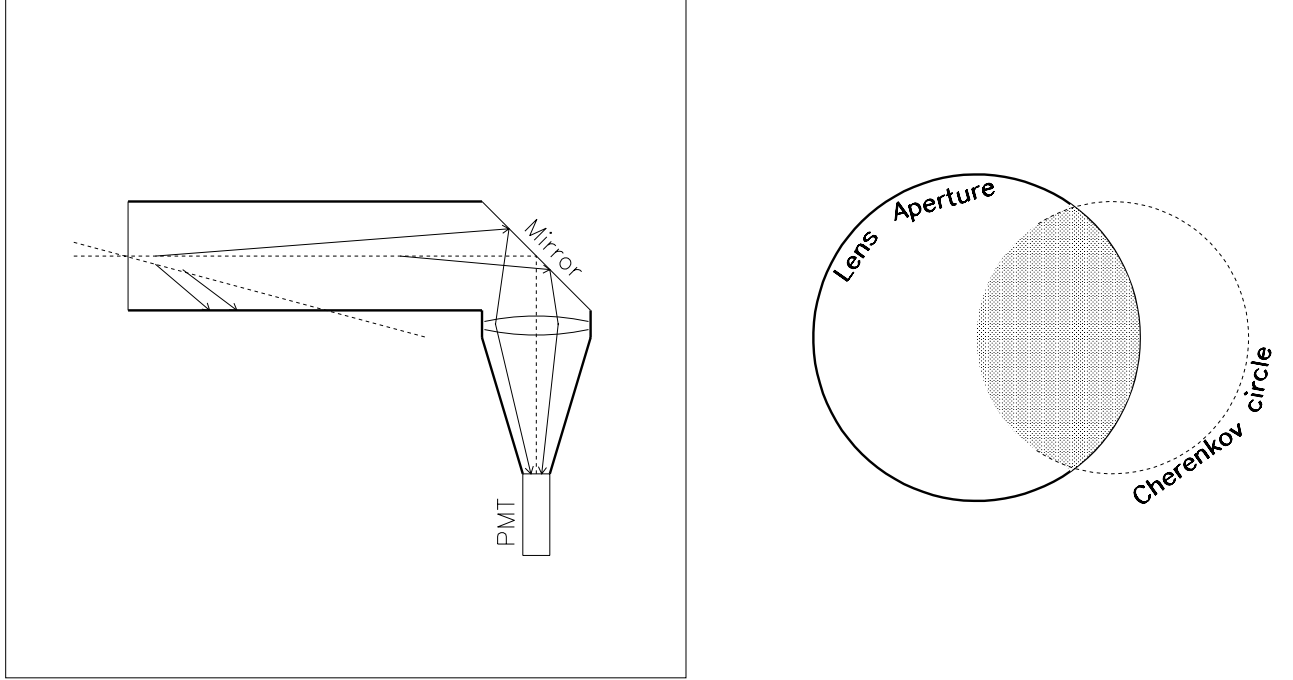


Figure 7: Left: Direction-selective gas Čerenkov counter. The light not touching black walls is focused by a lens onto a PMT. Right: Position of a Čerenkov light spot within the lens aperture for a non-parallel track.

- Čerenkov angle: $\Theta = \sqrt{2\eta} = 0.025$
- Threshold: $\gamma = 1/\sqrt{1 - 1/n^2} = 1/\sqrt{2\eta} = 1/\Theta = 40$
- Yield: $N_{p.e.} = 100/\text{cm} \cdot 100\text{cm} \cdot \Theta^2 = 10^4 \cdot 2\eta = 6$ photoelectrons

One may add directional selectivity to the counter by the design shown in Fig.7. The light emitted by a particle parallel to the axis does not touch wall and is focused by a lens onto a PMT. The light emitted by a large-angle particle is absorbed by the black counter's wall.

For a small angle the Čerenkov circle only partially overlaps with the lens aperture (Fig.7, right). Light collection efficiency calculated with this in mind is shown in Fig.8.

The rate is estimated to 300 MHz/cm^2 for the open hole and is saturated by electrons. Fig. 9 shows electron spectra (left) and heavy

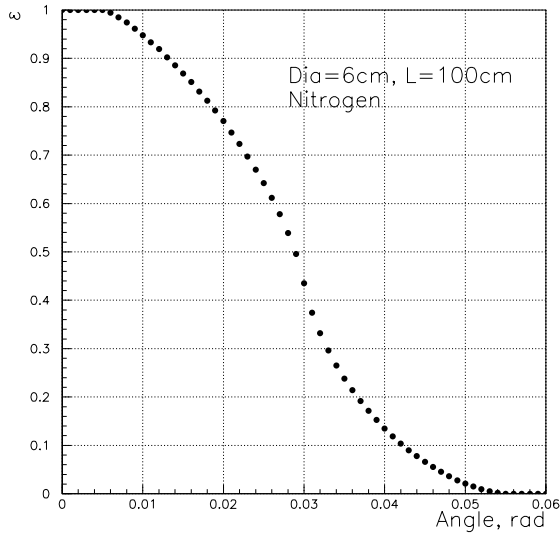


Figure 8: Light collection efficiency as a function of the incident angle for 6 cm dia, 1 m long counter filled with nitrogen at atmospheric pressure.

particles' (muon and heavier) spectra. Nothing much can be done to reduce the rate by using a gas other than nitrogen. Note that in terms of the photon yield 1 mm of PMT's window worth 1 m of nitrogen while window has much lower threshold. So the PMT face should be carefully shielded.

Fig. 10 shows the angular distribution of the electrons above threshold in shadowed histogram. The angle is measured between the electron's momentum and detector's axis. Large angles suggest that these electrons come from the secondary interactions in shielding. The distribution for the glass counter (fig.5, right) is superimposed for contrast.

Glass fiber counter looks preferable in rate, angular selectivity and simplicity.

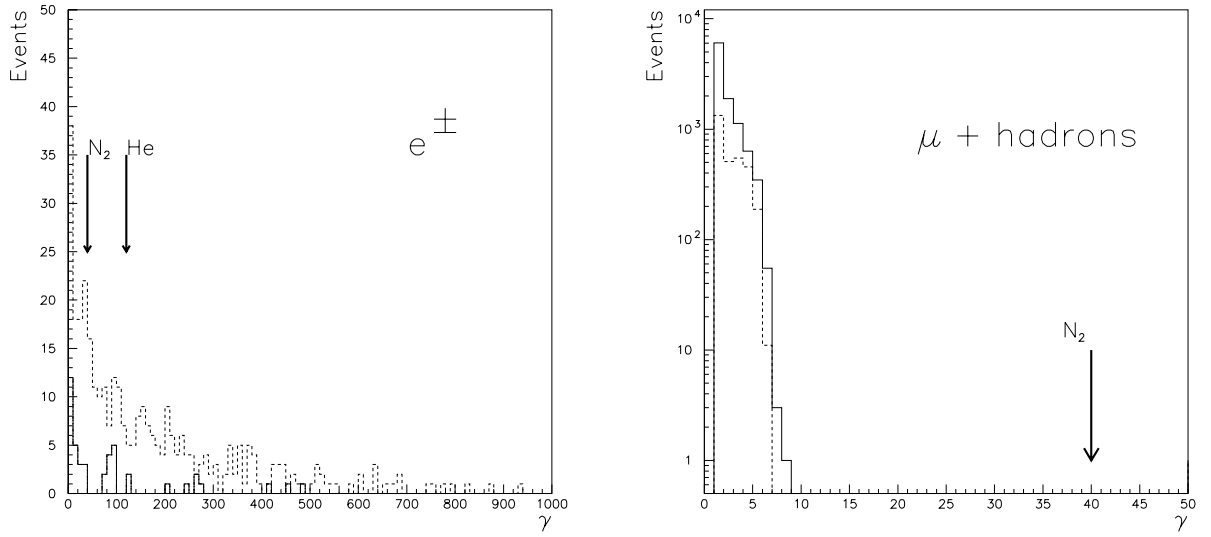


Figure 9: Spectra for open hole (solid line) and for 5 cm iron plug (dashed line), arrows indicate the thresholds in nitrogen and helium. Left: electrons, right: $\mu + \text{hadrons}$. Note how dramatically changes the proportion of electrons to hadrons when plugging a hole: 5 cm of iron ≈ 3 radiation lengths.

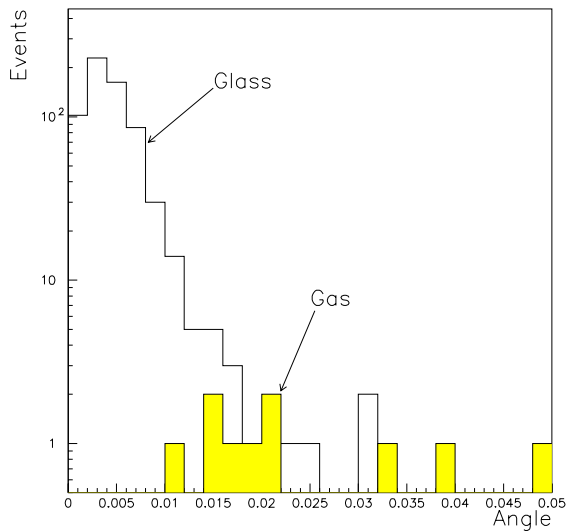


Figure 10: Angular distributions for the particles contributing to the gas Čerenkov signal ($\gamma > 40$, hatched histogram). Superimposed light histo is the distribution for the particles contributing to the glass counter signal (see fig.5, right). Neglect absolute normalisation, watch shape.

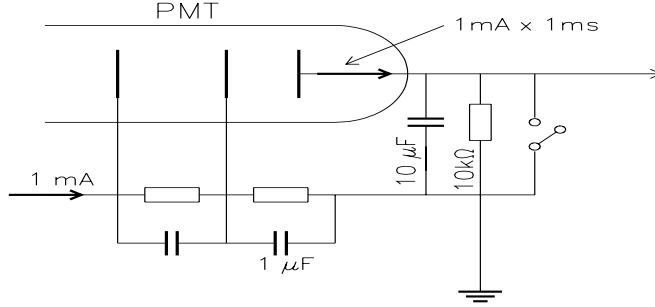


Figure 11: Integrating PMT output signal.

3 Integration Technique

Integrating the PMT output is much easier than integrating the target charge since the detector is exposed to far less radiation flux than the target is. This makes radiation strength problem bearable. Fig.11 shows the end of the PMT equipped for integration. The PMT may view Čerenkov or scintillator detector. For the numerical example let's assume 100 MHz particle rate, 100 photoelectrons per particle and PMT gain of $G=10^6$. Then the average cathode current is

$$\langle I_c \rangle = 10^8 \text{ Hz} \times 100 \text{ p.e.} \times 1.6 \cdot 10^{-19} = 1.6 \cdot 10^{-9} \text{ A} \approx 1 \text{ nA} \quad (6)$$

The average anode current then is $\langle I_a \rangle = \langle I_c \rangle \times G \approx 1 \text{ mA}$.

In 1 ms this makes 100 mV signal across 10 μF integrating capacitor. The discharge through the load resistor is negligible:

$$\tau = 10 \text{ k}\Omega \times 10 \mu\text{F} = 100 \text{ ms} \gg 1 \text{ ms} \quad (7)$$

The capacitor between the anode and the last dynode holds enough charge to support 1 mA anode current for 1 ms:

$$1\mu\text{F} \times 100\text{V} = 10^{-4}\text{C} \gg (1\text{mA} \times 1\text{ms} = 10^{-6}\text{C}) \quad (8)$$

This looks very simple and robust. However this technique is not direction-sensitive. What kind of detector works best with integration?

- Glass Čerenkov: there is no advantage of the amplitude discrimination any more. So it picks up a stuff at large angles which is not coming directly from the target
- Gas Čerenkov: has intrinsic suppression of large-angle tracks. However the signal is completely dominated by electrons which generally scatter more than muons and hadrons. There is no way to verify the origin of these electrons.
- Scintillator counter: all of the above problems apply plus soft stuff and neutrons.

Still is not as good as Glass Čerenkov with amplitude discrimination.

4 MC Technique

GEANT package has been used to estimate fluxes. Since detector occupies only a tiny solid angle, the straightforward application of GEANT is not effective. Two methods were used do resolve this problem.

4.1 Explicit hole simulation

The hole is explicitly implemented in geometry as shown in Fig.2. However, the interaction vertex is always translated to the interval $|Z| < \Delta Z$ and interaction products are rotated to fall into the interval $|\phi| < \Delta\phi$. The efficiency gain coefficients are given in Table 2 for 2.5

cm and 1 cm dia. holes. 1 meter long target assumed. One simulated event worth 3000 protons on target for 1 cm hole and 400 protons on target for 2.5 cm hole.

Table 2. Efficiency gain coefficients.

	1 cm dia.	2.5 cm dia.
ΔZ	± 0.5 cm	± 1.25 cm
$\Delta \phi$	$\pm \pi/30$	$\pm \pi/10$
Gain	3000	400
File	air_1cm_30fi	air_2.5cm_10fi
Events	$0.352 \cdot 10^6$	$0.569 \cdot 10^6$
1 event worth	37.8 MHz	175 MHz
	48 MHz/cm ²	35.7MHz/cm ²

4.2 Primary interaction approximation

Only the primary interaction in the target is simulated and then all the products allowed to travel pretending there is no any shield. Neglecting shield interactions gives the lower limit rate estimate¹. Since geometry now regains its azimuth symmetry, a set of multiple identical detectors implemented in GEANT geometry (Fig.12) provides a real huge simulation efficiency gain. Efficiency gains for detector diameters of 1 and 2 mm are represented in Table 3. Vertex translation in Z (see the paragraph above) is still in effect.

Table 3. Efficiency gain coefficients.

¹Don't get confused. Although eliminating the shielding increases the overall rate dramatically, the rate per cm² is lower than for the detector located at the end of a hole. In the latter case detector is exposed to both primary (directly from target) and secondary (from the hole's wall) radiation.

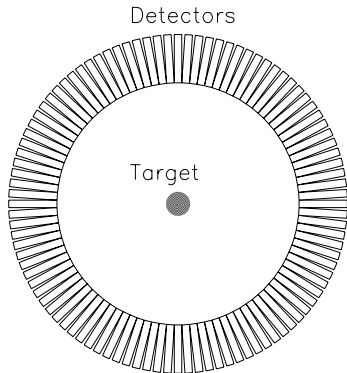


Figure 12: 'Porcupine' geometry; pretending multiple 90° detectors greatly increases effective number of proton interactions simulated.

	1 mm dia.	2 mm dia.
Segments in ϕ	10053	5026
Layers in Z	5	5
Detectors	50265	25130
ΔZ	± 2.5 mm	± 5 mm
Gain	$5 \cdot 10^6$	$2.5 \cdot 10^6$
File	yield_1_10	yield_2_10_plug5
Events	$1.115 \cdot 10^7$	$1.579 \cdot 10^7$
1 event worth	719 Hz	1016 Hz
	91.5 kHz/cm ²	32.3 kHz/cm ²

With such an efficiency the simulation of one full intensity spill ($4 \cdot 10^{13}$) comes to the simulation of 10^7 events. This, in turn, is quite practical (couple days at fsgi02) since tedious showering in the shielding avoided.

4.3 Comparison of two methods

Fig. 13, left represents the total charged flux calculations and shows an apparent difference between different methods. However, for fast

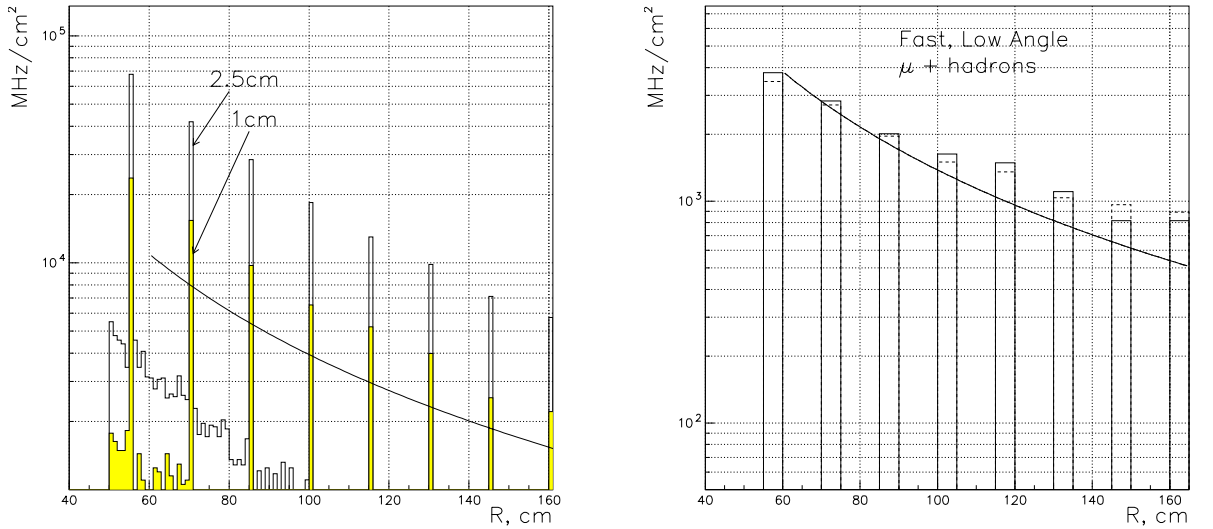


Figure 13: Left: Charged particles flux as a function of radius for 2.5 cm and 1 cm round holes. Line shows primary target interactions only scaled as $1/r^2$ and normalized at $R=160$ cm. Right: Same for the fast low-angle hadrons and muons: $\gamma > 2, \alpha < 20$ mrad. α stands for the angle between particle momentum and detector axis.

low-angle muons and hadrons, category responsible for the peak in the glass Čerenkov amplitude spectrum, (fig. 13, right) all methods give roughly the same result. Compare, for example, to the results for the electron flux. At $R=160$ cm the direct hole simulation gives about 750 and 200 MHz/cm^2 for 2.5 cm and 1 cm dia holes respectively while target interactions only gives 7.5 MHz/cm^2 .

Tables 1 through 3 have all the relevant technical details to convert number of events into rates.

Calculated by explicit hole simulation are: coloumn 'Open hole' of Table 1, shadowed histo in fig.10 and histograms in fig.13.

Calculated by primary interaction approximation are the distributions: figs.4,5,6,9, 'Glass' distribution in fig.10 and solid lines in fig.13. Coloumns '5 cm Plug' and '15 cm Plug' of Table 1 are also calculated by primary interaction approximation.

5 Conclusions

If I was given the responsibility to build and operate the NuMI target monitor, I would stick to the quartz fiber Čerenkov counter with 5 cm plug because of:

- Reasonable counting rate along with suppression of the secondary interactions may be achieved by simple amplitude discrimination of the single counter's signal.
- The peak in the amplitude spectrum is a nice reference for calibration.
- Both Čerenkov counters and amplitude discrimination technique are very well known in HEP and all necessary items are commercially available.
- Only small detector with one PMT has to stay in a no-access hot area. Reliability.
- Flux calculations are less model-dependent than in other cases considered through this paper.

Gas Čerenkov counter has much higher counting rate and not as good angular selectivity. To suppress the secondary interactions one may think of using two or more such counters in coincidence. The whole thing then becomes somewhat awkward mechanically (remember, each counter is 1 m long). Then it requires some gas system which can not be repaired because of hot radiation environment... It does not look as elegant and simple as 10 cm piece of fiber.

Budal technique lacks radiation hardness thus requiring a solid material study.

Integration of the anode signal tells too little about the direction. It is very likely that the signal will be dominated by secondary interactions.

References

- [1] K. Budal, CERN 67-17, CERN, Geneva, Switzerland, 1967
- [2] S.A.Belianchenko et al., “Study of photomultipliers radiation hardness”, Preprint IHEP 96-90, Protvino, Russia ,1996. Submitted to NIM
- [3] Quote from Hamamatsu engineer (unpublished).

Contents

1	Budal	1
2	Counting Technique	3
2.1	Plugging a hole	3
2.2	Glass Čerenkov Counter	5
2.2.1	Amplitude Spectrum	6
2.3	Phototubes	10
2.4	problems	11
2.5	Gas Čerenkov Counter	11
3	Integration Technique	15
4	MC Technique	16
4.1	Explicit hole simulation	16
4.2	Primary interaction approximation	17
4.3	Comparison of two methods	18
5	Conclusions	20